JACS
JOURNAL OF THE AMERICAN CHEMICAL SOCIETY
Communication
pubs.acs.org/JACS

# Dual Changes in Conformation and Optical Properties of Fluorophores within a Metal–Organic Framework during Framework Construction and Associated Sensing Event

Won Cho, Hee Jung Lee, Goeun Choi, Sora Choi, and Moonhyun Oh*

Department of Chemistry, Yonsei University, 134 Shinchon-dong, Seodaemun-gu, Seoul 120-749, Korea

Supporting Information

**ABSTRACT:** Microsized chemosensor particle (CPP-16, CPP means coordination polymer particle), which is made from a metal–organic framework (MOF), is synthesized using pyrene-functionalized organic building block. This building block contains three important parts, a framework construction part, a $Cu^{2+}$ detection part, and a fluorophore part. PXRD studies have revealed that CPP-16 has a 3D cubic structure of MOF-5. During both MOF formation and sensing event, fluorophores within CPP-16 undergo dual changes in conformation and optical properties. After MOF construction, pyrene moieties experience an unusual complete conversion from monomer to excimer form. This conversion takes place due to a confinement effect induced by space limitations within the MOF structure. The selective sensing ability of CPP-16 on $Cu^{2+}$ over many other metal ions is verified by emission spectra and is also visually identified by fluorescence microscopy images. Specific interaction of $Cu^{2+}$ with binding sites within CPP-16 causes a second conformational change of the fluorophores, where they change from stacked excimer (CPP-16) to quenched excimer states (CPP-16·$Cu^{2+}$).

There is great demand on the design and construction of chemosensors that can selectively and sensitively detect heavy metal ions like Pb, Hg, and Cu.[1−3] Over the past few decades, several platforms for $Cu^{2+}$ detection have been developed, including those based on organic chemosensors and those based on heterogeneous solid sensing materials.[4−9] Among such platforms, solid sensing materials might be particularly interesting; in addition to use in sensing, they might also be useful in removing analytes from solutions.

Porous coordination polymers or metal–organic frameworks (MOFs) are novel class of materials used in many practical applications, including gas storage, separation, catalysis, and recognition.[10−18] In general, MOF properties can be tuned through changes in pore structure and pore surface functionality. There has been recent immersing interest in nano- and microsized MOFs (or coordination polymer particles, CPPs) for the advanced utilization of them in gas storage, catalysis, and biological-system applications.[19−28] Other applications of interest include detection of vapors, organic molecules, anions, and cations.[29−39] Rational design of MOF materials such that binding sites are tailored to specifically interact with analytes is essential for selective recognition or sensing applications. Design strategies for binding sites include incorporating unsaturated Lewis acid metal sites[31,32] or immobilizing specific Lewis basic sites[8,33−35] within the MOF structures. Of the two, the latter is more difficult, and so sensing on the specific metal ions using MOF-based materials has been more challenging. While some research groups have succeeded in immobilizing Lewis basic sites such as free pyridyl and hydroxyl groups into MOFs for metal ion ($Cu^{2+}$ or $Fe^{3+}$) sensing, excellent selectivity on the specific metal ion over other metal ions has yet to be described.[33−35] Herein, we report a fluorescent turn-off chemosensor microparticle for $Cu^{2+}$ sensing based upon a functional MOF (CPP-16). In addition, we report interesting optical property changes and conformational adjustments of fluorophores within the MOF structure (from monomer to excimer to quenched excimer states) during framework construction and sensing event. CPP-16 displayed a highly selective and convenient sensing on $Cu^{2+}$ over many other metal ions. Furthermore, we found that the specific interaction of $Cu^{2+}$ with binding sites within CPP-16 caused dangled fluorophore groups to undergo conformation change, and the fluorophores to turn off. This is the first known demonstration for fluorescence signaling via conformational changes of pendent fluorophores embedded within MOFs during sensing.

The MOF-based microsized chemosensor was constructed from a pyrene-functionalized organic building block ($H_2L$), 2-(pyrene-1-carboxamido)terephthalic acid (Scheme 1). Two-step synthesis for $H_2L$ is described in Scheme S1. The first synthesis step was chlorination of 1-pyrenecarboxylic acid to generate 1-pyrenecarbonyl chloride. The second step was coupling of 1-

**Scheme 1. Schematic Representation for Turn-off Fluorescent Chemosensor of Microsized CPP-16 on $Cu^{2+}$**

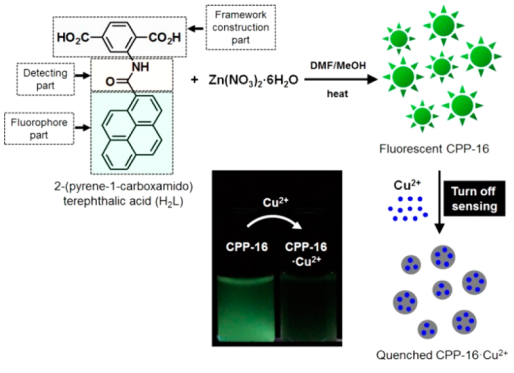


**Received:** April 28, 2014
**Published:** August 14, 2014

   dx.doi.org/10.1021/ja504204d | J. Am. Chem. Soc. 2014, 136, 12201−12204

pyrenecarbonyl chloride with 2-aminoterephthalic acid (Supporting Information (SI)). Isolated $H_2L$ was then fully characterized by $^1H$ NMR, $^{13}C$ NMR, IR, HR-Mass, and elemental analysis (SI). As shown in Scheme 1, the resulting $H_2L$ structure contains three vital parts: a terephthalic acid moiety for MOF-structure construction, a pyrene moiety for use a fluorophore, and an amide moiety for use in the metal ion's binding site. First, the reaction of $H_2L$ with $Zn(NO_3)_2$ will result in MOF formation as in a 3D cubic structure formation (MOF-5) from the reaction of terephthalic acid and $Zn(NO_3)_2$.[10,11] Second, $H_2L$ will be fluorescent due to the incorporation of a pyrene group within the molecule. Indeed, $H_2L$ shows typical monomeric emission bands of pyrene at 390 and 410 nm, when excited at 335 nm (Figure S2). Third, the resulting fluorescent $H_2L$ building blocks can potentially interact with specific metal ion through the amide group; specific binding of $Cu^{2+}$ via the nitrogen atom of the amide group has been well-known.[4−6]

Microsized CPP (CPP-16) for a fluorescent chemosensor was constructed from the following solvothermal reaction (Scheme 1). In the reaction, a precursor solution was prepared by mixing $Zn(NO_3)_2$ and $H_2L$ in *N*,*N*-dimethylformamide (DMF)/MeOH cosolvent. The resulting precursor solution was then heated at 110 °C for 40 min. The products formed were cooled to room temperature and isolated by centrifugation. The isolated products were then washed several times with fresh DMF and MeOH. The morphology of CPP-16 was first characterized by field-emission scanning electron microscopy (FE-SEM), optical microscopy (OM), and fluorescence microscopy (FM). The formation of spherical particles with an average size of 2.22 ± 0.31 $\mu$m was identified, as shown in SEM images (Figure 1a,c). In addition, high-magnification SEM image (Figure 1a inset) described in more detail the formation of particles containing many domains of MOF crystals. IR spectrum of CPP-16 confirmed coordination of the carboxylate groups of $L^{2-}$ to $Zn^{2+}$ ions, as evidenced by a shift in the CO stretching frequency to 1567 $cm^{-1}$ (Figure S3). Note that the original CO stretching frequency of the uncoordinated $H_2L$ was observed at 1692 $cm^{-1}$ (Figure S3). The chemical composition of CPP-16 was verified by energy dispersive X-ray (EDX) spectroscopy. The presence of organic ligands and zinc ions within CPP-16 was confirmed by detection of carbon, nitrogen, oxygen, and zinc atoms in EDX spectrum (Figure 1d). Resulting CPP-16 was found to be thermally stable up to 370 °C, as verified by thermogravimetric analysis (TGA, Figure 1e). A weight change (77.9%) observed in the TGA curve was comparable to the theoretical weight change (78.3%) calculated by the compositional change from $Zn_4OL_3$ (analogue of MOF-5; note that composition of MOF-5 is $Zn_4O(BDC)_3$) to ZnO.

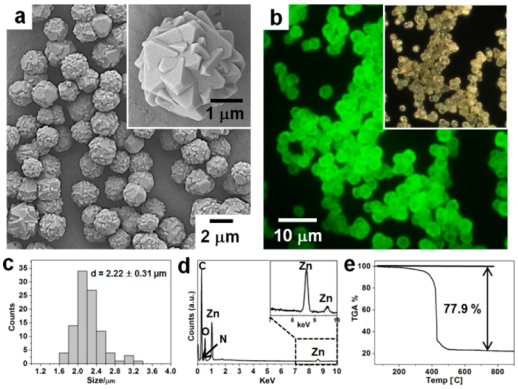


**Figure 1.** (a) Low- and high-magnification (inset) SEM images and (b) FM and OM (inset) images of microsized pyrene-functionalized CPP-16 with an average size of 2.22 ± 0.31 $\mu$m (SD, $n$ = 100), as determined by SEM. (c) Size distribution, (d) EDX spectrum, and (e) TGA curve of CPP-16.

CPP-16 was fluorescent, as a result of incorporation of fluorescent organic building blocks into the structure. Interestingly, all of the pyrene groups in CPP-16 were present in the excimer form. In general, the monomeric pyrene emission bands are shown at ∼370−430 nm; however, the excimer emission bands of pyrene are located at above 460 nm.[1,2,4,5] After CPP-16 formation, initial monomeric emission bands disappeared completely and new emission bands centered at 483 and 510 nm were only detected, when excited at 335 nm in MeCN suspension (Figure 2, black line). These new bands are attributed

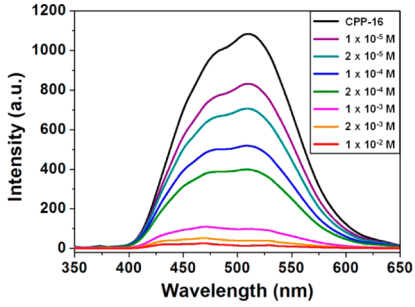


**Figure 2.** Fluorescence titration spectra of CPP-16 with addition of different concentrations of $Cu(NO_3)_2$ in MeCN. Excitation wavelength is 335 nm.

to excimer species of pyrene moieties, with overlapped pyrene units resulting in intramolecular $\pi-\pi$ stacking interactions.[1,4,5,40] This unique phenomenon of all pyrene moieties existing in excimer form without monomer form after MOF formation may be explained by a confinement effect. Specifically, as a result of the limited space within the MOF structure, dangled pyrene groups will be forced together, forming the excimer. This is a noteworthy discovery demonstrating an interesting confinement effect within the limited space of MOF, which causes a conformational change of pendent groups. The fluorescent CPP-16 was also identified by FM image (Figure 1b), where CPP-16 is fluorescent in the green region of spectrum.

Powder X-ray diffraction (PXRD) pattern was measured to obtain the structural information on CPP-16 (Figure 3e). Although with broad diffraction patterns, the PXRD pattern of CPP-16 was almost identical to that of the well-known MOF-5, obtained from $Zn^{2+}$ and terephthalic acid. Consequently, we concluded that CPP-16 has a 3D cubic structure of MOF-5 (Figure 3e inset). Moreover, there was a very broad extra diffraction peak (centered at $2\theta$ = 23.4°) in addition to the peaks attributed to the basic MOF-5 frame. This broad extra peak may have originated from stacked pyrene units. Note that a typical (002) diffraction peak of graphite carbon is observed at ca. $2\theta$ = 23−25°.[41,42]

The fluorescence titration of CPP-16 with $Cu^{2+}$ in MeCN revealed a decrease in fluorescence intensity of the pyrene excimer emission bands of CPP-16 with an increase in the amount of $Cu^{2+}$ (Figure 2). Decrease of the excimer emission bands possibly results from the interaction of $Cu^{2+}$ with CPP-16. Unfortunately, the exact interacting site of $Cu^{2+}$ within CPP-16 was not defined. Upon the basis of the literature,[4−6] we could


dx.doi.org/10.1021/ja504204d | J. Am. Chem. Soc. 2014, 136, 12201−12204

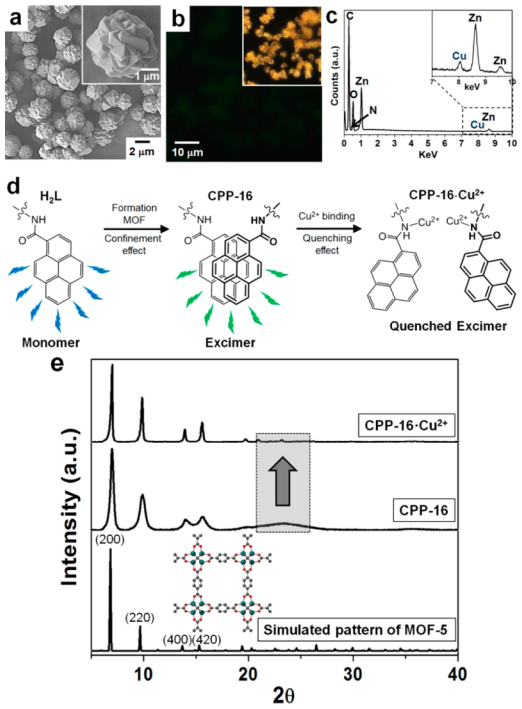


**Figure 3.** (a) Low- and high-magnification (inset) SEM images and (b) FM and OM (inset) images of CPP-16·$Cu^{2+}$. (c) EDX spectrum of CPP-16·$Cu^{2+}$. (d) Schematic representation showing the possible conformational changes during MOF formation (CPP-16) and interaction of $Cu^{2+}$ analytes with amide groups (CPP-16·$Cu^{2+}$). (e) Simulated PXRD pattern of MOF-5 (bottom), PXRD pattern of CPP-16 (middle), and PXRD pattern of CPP-16·$Cu^{2+}$ (top).

guess that $Cu^{2+}$ is possibly interacting with the nitrogen atoms of the amide groups within CPP-16. It was known that $Cu^{2+}$ is coordinated through the nitrogen atoms of the amide groups.[4−6] Kim et al. reported pyrene-functionalized calix[4]crown in which $Cu^{2+}$ interacts with the nitrogen atoms of the amide groups to form N−$Cu^{2+}$.[4] As speculated based upon the literature[4] (see CPP-16·$Cu^{2+}$ in Figure 3d), the pyrene groups may not have remained in excimer form (with parallel stacking of pyrene units) after coordination of $Cu^{2+}$ with amide groups. The broad diffraction peak in the PXRD pattern of CPP-16 at $2\theta$ = 23.4°, which may have originated from stacked pyrene units within CPP-16, completely disappeared at the PXRD pattern of CPP-16·$Cu^{2+}$ (Figure 3e top), which suggests the absence of stacked pyrene units as a result of conformational change. Figure 3e also describes how the observed PXRD pattern of CPP-16·$Cu^{2+}$ is almost identical to that of MOF-5. Even though the PXRD peaks of CPP-16 were somewhat broad, the PXRD peaks of CPP-16·$Cu^{2+}$ were quite sharp. Conceivably, the strain induced by the intramolecular $\pi-\pi$ stacking interaction of dangled pyrene groups in the case of CPP-16 may have resulted in the peak broadening, as opposed to having sharper peaks arising from strain release resulting from the lack of intramolecular $\pi-\pi$ stacking interactions within quenched excimer after interaction with $Cu^{2+}$.

The SEM image of CPP-16·$Cu^{2+}$ revealed that the original multidomain-crystallized morphology was maintained well after reaction with $Cu^{2+}$ (Figure 3a). Change in optical property of fluorescent chemosensor CPP-16 was easily recognized by FM image (Figure 3b), with the initial green emission (Figure 1b) of CPP-16 almost absent after interaction with $Cu^{2+}$. A photograph image obtained after the addition of $Cu^{2+}$ solution (after 10 s.) revealed the disappearance of the initial emission (Figure S4). Incorporation of $Cu^{2+}$ ions within CPP-16 was further verified by EDX spectrum analysis, as Cu atoms were detected, in addition to Zn, C, N, and O atoms (Figure 3c). $CO_2$ sorption isotherms of CPP-16 and CPP-16·$Cu^{2+}$ were measured at 195 K. $CO_2$ uptake abilities of CPP-16 (70 $cm^3g^{-1}$) decreased after the incorporation of $Cu^{2+}$ within CPP-16 to 51 $cm^3g^{-1}$ for CPP-16·$Cu^{2+}$ (Figure S5).

Selective sensing of CPP-16 on $Cu^{2+}$ has been validated by thorough observation of parallel relations using a variety of other metal ions in place of $Cu^{2+}$ (Figures 4 and S6). Specifically, CPP-

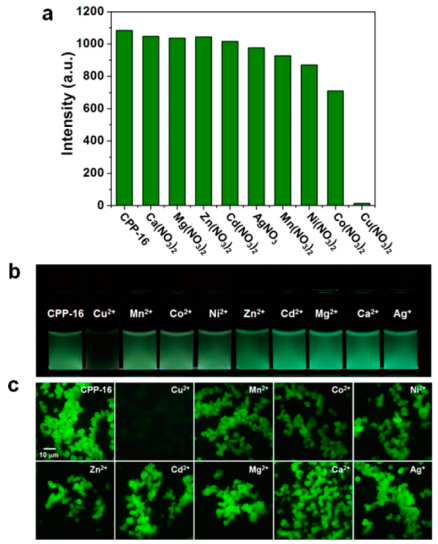


**Figure 4.** (a) Fluorescence intensity changes of CPP-16 after reaction with various metal ions (10 mM). (b) Digital photograph with UV irradiation and (c) FM images of a series of CPP-16 before and after reaction with various metal ions.

16 was immersed in several different kinds of MeCN solutions, which contained different kinds of metal ions, such as $Mg^{2+}$, $Ca^{2+}$, $Mn^{2+}$, $Co^{2+}$, $Ni^{2+}$, $Zn^{2+}$, $Ag^{+}$, and $Cd^{2+}$ (10 mM). Fluorescence intensity changes of CPP-16 following immersion in the various metal ion solutions were dependent on the specific identity of the metal ions (Figures 4a and S6). Alkaline-earth metal ions such as $Mg^{2+}$ and $Ca^{2+}$ had nearly no effect on the fluorescence intensity of the initial CPP-16. Moreover, little effect was found for transition metal ions such as $Mn^{2+}$, $Co^{2+}$, $Ni^{2+}$, $Zn^{2+}$, $Ag^{+}$, and $Cd^{2+}$. The only considerable quenching effect on CPP-16 fluorescence intensity was found for $Cu^{2+}$. Specifically, the quenching effect of metal ions was quantified by the Stern−Volmer equation[33,34] ($I_0/I = 1 + K_{sv}[M]$), where $I_0$ and $I$ are emission intensity of CPP-16 before and after reactions with metal ions, $K_{sv}$ is the quenching effect coefficient of the metal ions, and $[M]$ is the concentration of the metal ions. As shown in Table 1, the largest and distinguishable $K_{sv}$ value was obtained for $Cu^{2+}$ at 7846.7 $M^{-1}$. The selectivity on $Cu^{2+}$ was confirmed again by photograph showing the response of CPP-16 to various metal ions (Figure 4b). In addition, the selective response to metal ions was visualized by FM (Figure 4c). The influence of interrupting $Cu^{2+}$ sensing by other metal ions was studied by conducting $Cu^{2+}$ sensing in the presence of many other metal ions. Emission spectra (Figure S7) described no disturbance on selective $Cu^{2+}$ sensing by any of the other metal ions. Lastly, the green emission of the particles was recovered when they were washed using NaCN solution[43,44] (Figure S8).


dx.doi.org/10.1021/ja504204d | J. Am. Chem. Soc. 2014, 136, 12201−12204

**Table 1. Quenching Effect Coefficients ($K_{sv}$) of Various Metal Ions on the Fluorescence Intensity of CPP-16**

| metal ions | $K_{sv}$ [$M^{-1}$] | metal ions | $K_{sv}$ [$M^{-1}$] |
|---|---|---|---|
| $Ca^{2+}$ | 3.4 | $Mn^{2+}$ | 17.0 |
| $Mg^{2+}$ | 4.6 | $Ni^{2+}$ | 24.4 |
| $Zn^{2+}$ | 3.9 | $Co^{2+}$ | 52.7 |
| $Cd^{2+}$ | 6.7 | $Cu^{2+}$ | 7846.7 |
| $Ag^{+}$ | 10.9 | | |

In conclusion, we developed a pyrene-functionalized CPP-16 that is an efficient and convenient fluorescent chemosensor for $Cu^{2+}$ detection. The synthesized organic building block ($H_2L$) consists of three vital parts, a frame part for MOF construction, a fluorophore part for signaling, and a binding component for $Cu^{2+}$ detection. We found complete conversion of the dangled pyrene groups from the monomer form in the case of free $H_2L$ to the excimer form in CPP-16 to be the result of a confinement effect, induced by the limited space within the MOF. Selective interaction of CPP-16 with $Cu^{2+}$ over many other metal ions was verified by selective trun-off sensing by $Cu^{2+}$. Significant decrease of CPP-16 fluorescence intensity was observed upon CPP-16 interaction with $Cu^{2+}$, but not other metals. Specific interaction of $Cu^{2+}$ with CPP-16 resulted in change of the dangled pyrene groups from the stacked excimer state to the quenched excimer state.

## ■ ASSOCIATED CONTENT

### Supporting Information

Experimental details, and characterization data. This material is available free of charge via the Internet at http://pubs.acs.org.

## ■ AUTHOR INFORMATION


### Corresponding Author

moh@yonsei.ac.kr


### Notes

The authors declare no competing financial interest.

## ■ ACKNOWLEDGMENTS

This work was supported by the National Leading Research Lab Program (no. NRF-2012R1A2A1A03670409) through NRF grant funded by the Ministry of Science, ICT and Future Planning.

## ■ REFERENCES


(1) Kim, S. K.; Lee, S. H.; Lee, J. Y.; Lee, J. Y.; Bartsch, R. A.; Kim, J. S. *J. Am. Chem. Soc.* **2004**, *126*, 16499.

(2) Caballero, A.; Martinez, R.; Lloveras, V.; Ratera, I.; Vidal-Gancedo, J.; Wurst, K.; Tárraga, A.; Molina, P.; Veciana, J. *J. Am. Chem. Soc.* **2005**, *127*, 15666.

(3) Hennrich, G.; Walther, W.; Resch-Genger, U.; Sonnenschein, H. *Inorg. Chem.* **2001**, *40*, 641.

(4) Choi, J. K.; Kim, S. H.; Yoon, J.; Lee, K.-H.; Bartsch, R. A.; Kim, J. S. *J. Org. Chem.* **2006**, *71*, 8011.

(5) Jung, H. S.; Park, M.; Han, D. Y.; Kim, E.; Lee, C.; Ham, S.; Kim, J. S. *Org. Lett.* **2009**, *11*, 3378.

(6) Zheng, Y.; Cao, X.; Orbulescu, J.; Konka, V.; Andreopoulos, F. M.; Pham, S. M.; Leblanc, R. M. *Anal. Chem.* **2003**, *75*, 1706.

(7) Basabe-Desmonts, L.; Beld, J.; Zimmerman, R. S.; Hernando, J.; Mela, P.; García Parajó, M. F.; van Hulst, N. F.; van den Berg, A.; Reinhoudt, D. N.; Crego-Calama, M. *J. Am. Chem. Soc.* **2004**, *126*, 7293.

(8) Liu, S.; Xiang, Z.; Hu, Z.; Zheng, X.; Cao, D. *J. Mater. Chem.* **2011**, *21*, 6649.

(9) Xiao, Y.; Cui, Y.; Zheng, Q.; Xiang, S.; Qian, G.; Chen, B. *Chem. Commun.* **2010**, *46*, 5503.

(10) Li, H.; Eddaoudi, M.; O'Keeffe, M.; Yaghi, O. M. *Nature* **1999**, *402*, 276.

(11) Eddaoudi, M.; Kim, J.; Rosi, N.; Vodak, D.; Wachter, J.; O'Keeffe, M.; Yaghi, O. M. *Science* **2002**, *295*, 469.

(12) Liu, B.; Tu, M.; Fischer, R. A. *Angew. Chem., Int. Ed.* **2013**, *52*, 3402.

(13) Maji, T. K.; Matsuda, R.; Kitagawa, S. *Nat. Mater.* **2007**, *6*, 142.

(14) Herm, Z. R.; Wiers, B. M.; Mason, J. A.; van Baten, J. M.; Hudson, M. R.; Zajdel, P.; Brown, C. M.; Masciocchi, N.; Krishna, R.; Long, J. R. *Science* **2013**, *340*, 960.

(15) Bohnsack, A. M.; Ibarra, I. A.; Bakhmutov, V. I.; Lynch, V. M.; Humphrey, S. M. *J. Am. Chem. Soc.* **2013**, *135*, 16038.

(16) Karagiaridi, O.; Lalonde, M. B.; Bury, W.; Sarjeant, A. A.; Farha, O. K.; Hupp, J. T. *J. Am. Chem. Soc.* **2012**, *134*, 18790.

(17) Wanderley, M. M.; Wang, C.; Wu, C.-D.; Lin, W. *J. Am. Chem. Soc.* **2012**, *134*, 9050.

(18) Férey, G.; Haouas, M.; Loiseau, T.; Taulelle, F. *Chem. Mater.* **2014**, *26*, 299.

(19) Oh, M.; Mirkin, C. A. *Nature* **2005**, *438*, 651.

(20) Cho, W.; Lee, H. J.; Oh, M. *J. Am. Chem. Soc.* **2008**, *130*, 16943.

(21) Jung, S.; Cho, W.; Lee, H. J.; Oh, M. *Angew. Chem., Int. Ed.* **2009**, *48*, 1459.

(22) Li, T.; Sullivan, J. E.; Rosi, N. L. *J. Am. Chem. Soc.* **2013**, *135*, 9984.

(23) Pullen, S.; Fei, H.; Orthaber, A.; Cohen, S. M.; Ott, S. *J. Am. Chem. Soc.* **2013**, *135*, 16997.

(24) Foucault-Collet, A.; Gogick, K. A.; White, K. A.; Villette, S.; Pallier, A.; Collet, G.; Kieda, C.; Li, T.; Geib, S. J.; Rosi, N. L.; Petoud, S. *Proc. Natl. Acad. Sci. U.S.A.* **2013**, *110*, 17199.

(25) Lin, W.; Rieter, W. J.; Taylor, K. M. L. *Angew. Chem., Int. Ed.* **2009**, *48*, 650.

(26) Spokoyny, A. M.; Kim, D.; Sumrein, A.; Mirkin, C. A. *Chem. Soc. Rev.* **2009**, *38*, 1218.

(27) Rocca, J. D.; Liu, D.; Lin, W. *Acc. Chem. Res.* **2011**, *44*, 957.

(28) Carné, A.; Carbonell, C.; Imaz, I.; Maspoch, D. *Chem. Soc. Rev.* **2011**, *40*, 291.

(29) Nagarkar, S. S.; Joarder, B.; Chaudhari, A. K.; Mukherjee, S.; Ghosh, S. K. *Angew. Chem., Int. Ed.* **2013**, *52*, 2881.

(30) Chen, B.; Wang, L.; Zapata, F.; Qian, G.; Lobkovsky, E. B. *J. Am. Chem. Soc.* **2008**, *130*, 6718.

(31) Li, Y.; Zhang, S.; Song, D. *Angew. Chem., Int. Ed.* **2013**, *52*, 710.

(32) Chen, B.; Yang, Y.; Zapata, F.; Lin, G.; Qian, G.; Lobkovsky, E. B. *Adv. Mater.* **2007**, *19*, 1693.

(33) Jayaramulu, K.; Narayanan, R. P.; George, S. J.; Maji, T. K. *Inorg. Chem.* **2012**, *51*, 10089.

(34) Chen, B.; Wang, L.; Xiao, Y.; Fronczek, F. R.; Xue, M.; Cui, Y.; Qian, G. *Angew. Chem., Int. Ed.* **2009**, *48*, 500.

(35) Tang, Q.; Liu, S.; Liu, Y.; Miao, J.; Li, S.; Zhang, L.; Shi, Z.; Zheng, Z. *Inorg. Chem.* **2013**, *52*, 2799.

(36) Kreno, L. E.; Leong, K.; Farha, O. K.; Allendorf, M.; Van Duyne, R. P.; Hupp, J. T. *Chem. Rev.* **2012**, *112*, 1105.

(37) Evans, J. D.; Sumby, C. J.; Doonan, C. J. *Chem. Soc. Rev.* **2014**, *43*, 5933.

(38) Park, J.; Sun, L.-B.; Chen, Y.-P.; Perry, Z.; Zhou, H.-C. *Angew. Chem., Int. Ed.* **2014**, *53*, 5842.

(39) Jiang, H.-L.; Feng, D.; Wang, K.; Gu, Z.-Y.; Wei, Z.; Chen, Y.-P.; Zhou, H.-C. *J. Am. Chem. Soc.* **2013**, *135*, 13934.

(40) Winnik, F. M. *Chem. Rev.* **1993**, *93*, 587.

(41) Wang, Q.; Xia, W.; Guo, W.; An, L.; Xia, D.; Zou, R. *Chem.—Asian J.* **2013**, *8*, 1879.

(42) Liu, B.; Shioyama, H.; Akita, T.; Xu, Q. *J. Am. Chem. Soc.* **2008**, *130*, 5390.

(43) Zeng, Q.; Cai, P.; Li, Z.; Qin, J.; Tang, B. Z. *Chem. Commun.* **2008**, 1094.

(44) Jung, H. S.; Han, J. H.; Kim, Z. H.; Kang, C.; Kim, J. S. *Org. Lett.* **2011**, *13*, 5056.